Journal of Statistical Physics, Vol. 61, Nos. 5/6, 1990

Lyapunov Exponents of Large, Sparse Random Matrices and the Problem of Directed Polymers with Complex Random Weights

J. Cook[1,2] **and B. Derrida**[1,3]

Received April 17, 1990; final July 11, 1990

We present results on two different problems: the Lyapunov exponent of large, sparse random matrices and the problem of polymers on a Cayley tree with random complex weights. We give an analytic expression for the largest Lyapunov exponent of products of random sparse matrices, with random elements located at random positions in the matrix. This expression is obtained through an analogy with the problem of random directed polymers on a Cayley tree (i.e., in the mean field limit), which itself can be solved using its relationship with random energy models (REM and GREM). For the random polymer problem with complex weights we find that, in addition to the high- and the low-temperature phases which were already known in the case of positive weights, the mean field theory predicts a new phase (phase III) which is dominated by interference effects.

KEY WORDS: Lyapunov exponent; directed polymer; interference; localization.

1. INTRODUCTION

It has been known, since the famous work of Wigner[1] and Dyson,[2] that the properties of large random $N \times N$ matrices can be described by analytic methods.[3] Properties such as the density of eigenvalues of large $N \times N$ matrices, the elements of which are randomly distributed, can be calculated analytically in the large-N limit, giving rise to the well-known semicircular law.

Frequently, products of random matrices arise in the study of disordered

[1] Service de Physique Théorique, CEN Saclay, F-91191 Gif-sur-Yvette, France.
[2] Department of Physics, University of Edinburgh, Edinburgh EH9 3JZ, United Kingdom.
[3] School of Mathematics, Institute for Advanced Study, Princeton, New Jersey 08540.

822/61/5-6-1

systems or dynamical systems[3–7] and one needs to evaluate the Lyapunov exponents of these products. Except in some limiting cases[8] or particular examples,[9] it is not known in general how to calculate Lyapunov exponents analytically.

Recently Newman[10,11] considered the problem of calculating the Lyapunov exponents of products of large $N \times N$ matrices. For finite N, he was able to give a closed expression for all the Lyapunov exponents when the matrix elements were distributed according to a Gaussian distribution. In addition, in the limit of large matrices ($N \to \infty$), he obtained the density of Lyapunov exponents for elements distributed according to an arbitrary distribution. In this paper we seek to extend the consideration of products of large random matrices to the case of sparse matrices and we present an expression for the largest Lyapunov exponent of such large, sparse, real matrices, the nonzero elements of which are chosen from an arbitrary distribution. The result is obtained by utilizing a close connection between this problem of random matrices and another problem in the theory of disordered systems, that of directed polymers in a random medium.[12–18]

The problem of directed polymers in a random medium is presently an active area of research in the theory of disordered systems. Much progress has been made on the problem both by analytical[13–17] and numerical techniques.[18] Recently a generalized version of the problem has been introduced[19–21] (where the statistical weights of the polymers are no longer all positive) as having possible relevance to hopping conductivity in random media. In this work we look at this generalized version of the problem and present results on its mean field solution.

In order to present our findings and discussions of several different problems in a clearer way, we shall first discuss our results (in Sections 2 and 3) and then later explain how they can be obtained (Sections 4–6). The paper is therefore arranged as follows. In Section 2 we define the random matrix problem that we shall consider and give the analytic expression for the largest Lyapunov exponent. Depending on the number of nonzero elements per row and on the probability distribution of these elements, we shall see that three possible cases can occur, each case corresponding to a different analytic expression for the largest Lyapunov exponent. These expressions are compared with the results of numerical simulations for several examples.

In Section 3, we define a version of the directed polymer problem (where the weight of each path can be either positive or negative) and give its mean field solution. We obtain three possible phases: in addition to the high-temperature and the low-temperature phase already known in the case of a polymer with positive weights, we find a new phase dominated by interference effects.

In Section 4 we begin the discussion of how our results were obtained. The expressions given in Sections 2 and 3 follow from the close relationships between four different problems of statistical mechanics: the Lyapunov exponent of large, random, sparse matrices, directed polymers in a random medium, the generalized random energy model (GREM),[22,23] and the random energy model (REM).[24–26] These four problems have the same phase diagram. In Sections 5 and 6, respectively, we show how one can solve versions of the REM and GREM, which provide us, via the links discussed in Section 4, with the main results of this paper.

2. THE LARGEST LYAPUNOV EXPONENT OF A PRODUCT OF LARGE, SPARSE, RANDOM MATRICES

Consider random matrices, of size $N \times N$, with K nonzero real elements in each row. Let the positions of the K nonzero elements be selected at random, each position being equally likely, and let each nonzero element x be chosen according to a given probability distribution $g(x)$. If one fixes K, but allows N to become very large ($N \to \infty$), it is possible to calculate the largest Lyapunov exponent γ of a product of such matrices. It is found that there are three possible cases, depending upon the choice of the distribution $g(x)$.

It is convenient to define a function $G(\lambda)$ as

$$G(\lambda) = \frac{1}{\lambda} \log \left[K \int_{-\infty}^{\infty} g(x) |x|^{\lambda} \, dx \right] \tag{1}$$

and to define $\lambda_{\min}$ to be the value of λ that minimizes $G(\lambda)$. For a given distribution $g(x)$, the largest Lyapunov exponent γ is given by

$$\gamma = \gamma_{\mathrm{II}} \qquad \text{if} \quad \lambda_{\min} \leqslant 1 \tag{2}$$

$$\gamma = \max(\gamma_{\mathrm{I}}, \gamma_{\mathrm{II}}) \qquad \text{if} \quad 1 \leqslant \lambda_{\min} \leqslant 2 \tag{3}$$

$$\gamma = \max(\gamma_{\mathrm{I}}, \gamma_{\mathrm{III}}) \qquad \text{if} \quad 2 \leqslant \lambda_{\min} \tag{4}$$

where γ_{I}, γ_{II}, and γ_{III} are

$$\gamma_{\mathrm{I}} = \log \left[K \left| \int_{-\infty}^{+\infty} g(x) x \, dx \right| \right] \tag{5}$$

$$\gamma_{\mathrm{II}} = G(\lambda_{\min}) \tag{6}$$

$$\gamma_{\mathrm{III}} = G(2) \tag{7}$$

To avoid some difficulties which would arise for some $g(x)$ which contain δ functions, we will exclude such distributions, requiring that $g(x)$ contains

no delta function. [For example, if $g(x) = (1-p)\,\delta(x+1) + p\delta(x-1)$ and $K=2$, it is easy to construct pairs of matrices M_1 and M_2 which occur with some nonzero probability, such that $M_1 M_2 = 0$.]

Let us first compare these analytic predictions for γ with the results of numerical simulations for three different examples (Fig. 1):

$$\text{Example 1:} \quad g(x) = 1 \quad \text{if} \quad a \leqslant x \leqslant 1+a$$
$$= 0 \quad \text{otherwise} \tag{8}$$

$$\text{Example 2:} \quad g(x) = ax^{-(a+1)} \quad x \geqslant 1$$
$$= 0 \quad x < 1 \tag{9}$$

$$\text{Example 3:} \quad g(x) = \tfrac{1}{2}a|x|^{-(a+1)} \quad |x| \geqslant 1$$
$$= 0 \quad |x| < 1 \tag{10}$$

For each of these examples, we calculated the largest Lyapunov exponent for three matrix sizes $N=1$, 100, and 10,000 by performing the product of 5×10^5 (for $N=1$), 5×10^4 (for $N=100$), and 5×10^3 (for $N=10{,}000$) random matrices. We always kept the number of elements K in each row to be $K=4$.

We chose the positions $i_1, i_2, \ldots, i_K$ of the K nonzero elements of each row at random. When two elements occurred at the same location, they were added (in particular, for $N=1$, we always had $i_1 = i_2 = i_3 = i_4 = 1$).

The results of the simulations for these three examples are shown in Fig. 2, together with the analytical expressions of γ obtained from Eqs. (2)–(7).

For example 1 [see Eq. (8)] we see in Fig. 2a that there is a transition at $a = -1/3$. Below this value of a, the numerical results converge rapidly with increasing N to γ_{III} [Eq. (7)], whereas above it, they converge rapidly toward γ_{I}. This agrees with the theoretical prediction. For this choice of

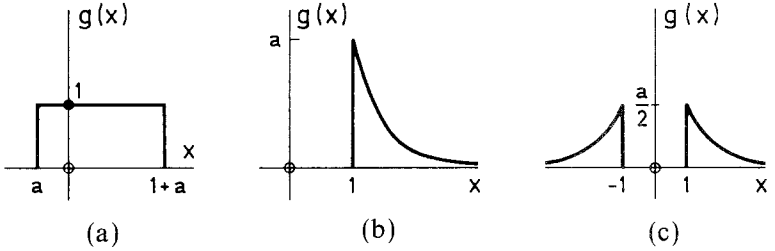

Fig. 1. The distributions $g(x)$ used to calculate the Lyapunov exponents in the numerical simulations shown in Fig. 2. (a) Eq. (8); (b) Eq. (9); (c) Eq. (10).

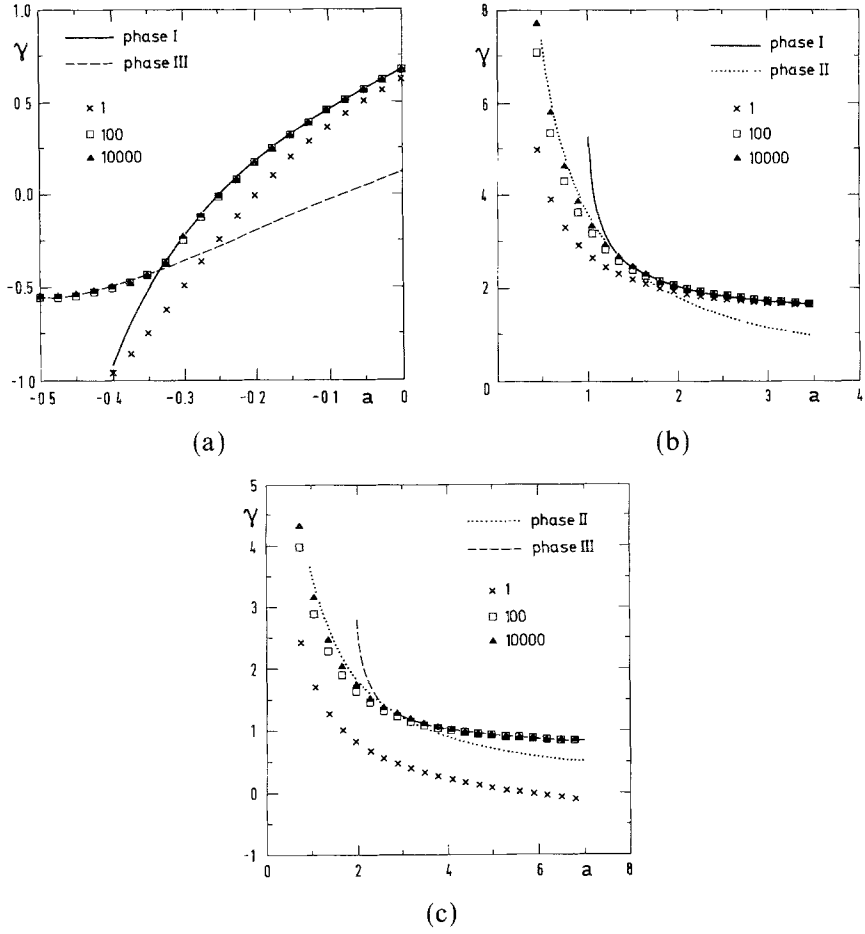

Fig. 2. The largest Lyapunov exponent γ plotted against the parameter a for the distributions $g(x)$ in (a) Fig. 1a, (b) Fig. 1b, (c) Fig. 1c. The curves show the analytical results [–, γ_I; Eq. (5); ···, γ_{II}, Eq. (6); - -, γ_{III}, Eq. (7)] and the points show the numerical data for system sizes $N = 1$, 100, 10,000.

$g(x)$, Eq. (8), one always finds $\lambda_{\min} > 2$ and so one expects only to observe cases I and III.

To observe case II, we had to choose other distributions $g(x)$ that give a value $\lambda_{\min} < 2$ [Eqs. (9) and (10)]. In the case of distribution (9), Eqs. (2)–(7) predict a transition between case II and case I as a is increased. This can be clearly seen from the numerical data in Fig. 2b, where the analytic expressions (5) and (6) are also shown. For large values

of the parameter a the results converge rapidly toward γ_{I}, and below $a \simeq 1.37$ the results converge toward γ_{II}, although the convergence is notably poorer in this case.

Lastly we considered a power-law distribution, symmetric about $x = 0$ [see Eq. (10)]. Clearly, one does not expect to observe case I now, as from (2) one sees that $\gamma_{\mathrm{I}} = -\infty$. The numerical results are shown in Fig. 2c together with the analytic expressions for II and III [Eqs. (6) and (7)]. For large enough a the numerical data converge rapidly toward γ_{III}, whereas below $a \simeq 2.74$ they converge toward γ_{II} with a slower convergence rate.

So, the simulations agree well with our analytical predictions [Eqs. (2)–(7)]. The convergence of the data toward the theoretical predictions as one increases the matrix size N is very rapid in cases I and III and clear, but notably slower in case II. It would be interesting to be able to understand these rates of convergence, but at present we are not able to do this. [We only have an argument which would give that it always converges faster than $\log(\log N)/\log N$.]

Finally, in this section let us point out one situation in which such $N \times N$ sparse matrices arise. Consider a geometry in which one has a series of L layers, each layer composed of N points (see Fig. 3). We shall label the points by integers n ($n = 1, 2, \ldots, N$). Suppose that each point in layer l is connected to K points in layer $l+1$, these K points being chosen at random from the N possible points. So there are KN bonds between layers l and $l+1$. We shall now consider a directed polymer problem in such a geometry. For each of the randomly selected bonds ij between adjacent layers one chooses a random energy ε_{ij} from a given distribution $\rho(\varepsilon_{ij})$ and a sign S_{ij} chosen to be positive with probability $1-p$ and negative with probability p ($0 \leqslant p \leqslant 1$). One then wants to consider all the walks passing through one point in each layer that can be formed using the random bonds. The energy of such walk ω is taken to be the sum of the energies on the bonds that it visits and the sign of the walk ω is the product of the

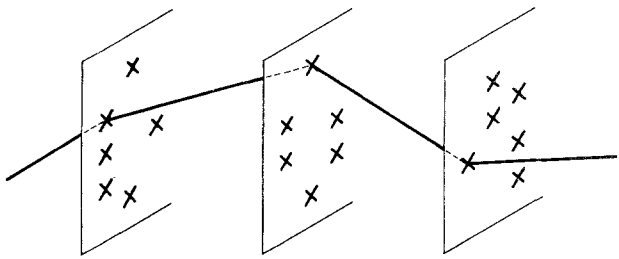

Fig. 3. The layered geometry of the directed polymer problem discussed in Section 2.

signs S_{ij} of the bonds visited. One can then define a kind of partition sum $Z_L(n)$ by

$$Z_L(n) = \sum_{\omega} \prod_{ij \in \omega} (S_{ij} e^{-\varepsilon_{ij}/T}) \tag{11}$$

where the sum runs over all walks of length L emanating from the point n in layer L, and the product includes all bonds that are visited by walk ω. Here T is the temperature. One can then write a recursion for Z_L,

$$Z_{L+1}(n) = \sum_{m=1}^{N} S_{nm} e^{-\varepsilon_{nm}/T} Z_L(m) \tag{12}$$

Hence the vector $\{Z_{L+1}\}$ is simply obtained from $\{Z_L\}$ by multiplication by an $N \times N$ matrix with K nonzero random elements in each row. One then clearly has a problem involving a product of random matrices of the type defined at the beginning of this section. This connection between the random matrix problem and directed polymers will be discussed further in Section 4.

3. DIRECTED POLYMERS IN A RANDOM MEDIUM: MEAN FIELD THEORY

In this section we present the mean field solution of a generalized version[21] of the problem of directed polymers in a random medium. First let us define the problem. One has some regular lattice and for each bond ij of the lattice a random energy ε_{ij} is chosen according to a given probability distribution $\rho(\varepsilon_{ij})$. Also, one places a random sign S_{ij} on each bond, taken to be positive with probability $1-p$ and negative with probability p. One then considers all directed walks ω emanating from some origin. By directed walk we mean a walk for which one selected coordinate is an increasing function of the length of the walk. One defines the energy E_ω of such a directed walk ω to be the sum of the energies on the bonds visited by that walk

$$E_\omega = \sum_{ij \in \omega} \varepsilon_{ij} \tag{13}$$

The "partition function" of the problem is then taken to be

$$Z_L(\mathbf{r}) = \sum_{\omega} \left(\prod_{ij \in \omega} S_{ij} \right) \exp(-E_\omega/T) \tag{14}$$

where the sum runs over all directed walks ω of length L emanating from the point $\mathbf{r}$ and T is the temperature. Although we shall call $Z_L(\mathbf{r})$ a partition

function, it can be positive or negative, due to the inclusion of random signs in the problem. In calculating the "thermal" properties of the system, to obtain the phase diagram, one is therefore interested in evaluating the quantity $\langle \log|Z_L| \rangle$ (where $\langle \cdot \rangle$ denotes an average over disorder). Notice that the standard directed polymer problem (see, for example, refs. 12–18) is recovered if $p=0$ or 1.

$Z_L(\mathbf{r})$ is the sum of contributions from all the paths of length L which reach the point $\mathbf{r}$. This can be viewed as the amplitude resulting from the transmission of a plane wave through a random medium.

The results we present below apply to the mean field limit of this generalized polymer problem, i.e., when one takes the underlying lattice to be a branch of a Cayley tree with branching ratio K (see Fig. 4). One then places a randomly-chosen energy and sign on each branch of the tree and considers all the walks running down the tree that originate at the root (the point 0 in Fig. 4). The standard directed polymer problem, i.e., when $p=0$ or 1, has already been solved in this mean field limit for an arbitrary distribution of energies $\rho(\varepsilon)$ and branching ratio K.[15] One finds two phases: a high-temperature phase in which the quenched and annealed free energies are equal

$$\lim_{L\to\infty} \left\langle \frac{\log|Z_L|}{L} \right\rangle = \lim_{L\to\infty} \frac{\log|\langle Z_L \rangle|}{L}; \qquad p=0 \text{ or } 1 \tag{15}$$

and a low-temperature frozen phase in which the partition sum is dominated by a finite number of walks.

When one allows p to vary, one obtains (see Sections 4–6) three phases. First there is a high-temperature phase, which we shall label phase I, which is very like the high-temperature phase in the $p=0$ or 1 problem. In this phase the quenched and annealed free energies are equal, in the sense that

$$\lim_{L\to\infty} \frac{\langle \log|Z_L(T)| \rangle}{L} = \lim_{L\to\infty} \frac{\log|\langle Z_L(T) \rangle|}{L} \tag{16}$$

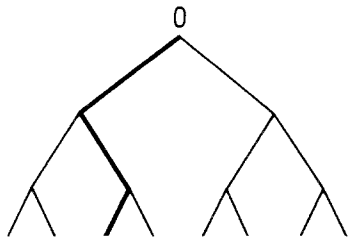

Fig. 4. A branch of a Cayley tree with branching ratio $K=2$. One directed walk emanating from the root, 0, is shown is bold.

Second there remains a low-temperature phase of the same character as at $p=0$. This is to be expected, as one knows that the partition sum is then dominated by a small number of walks and so the addition of random signs is unlikely to lead to any dramatic interference effects. We shall label this low-temperature phase, phase II. Lastly there appears a new phase, phase III. This is a high-temperature phase in which interference effects between walks with similar energies but opposite signs are important.

Let us now give expressions for $\langle \log|Z_L| \rangle / L$ in each of these phases, in terms of the branching ratio K, the energy distribution $\rho(\varepsilon)$, and the parameter p.

Phase I:

$$\lim_{L\to\infty} \frac{\langle \log|Z_L| \rangle}{L} = \log\left[K \int \rho(\varepsilon) e^{-\varepsilon/T}\, d\varepsilon\right] + \log[|1-2p|] \tag{17}$$

Phase II:

$$\lim_{L\to\infty} \frac{\langle \log|Z_L| \rangle}{L} = \min_{\lambda} \frac{1}{\lambda} \log\left[K \int \rho(\varepsilon) e^{-\varepsilon\lambda/T}\, d\varepsilon\right] \tag{18}$$

Phase III:

$$\lim_{L\to\infty} \frac{\langle \log|Z_L| \rangle}{L} = \frac{1}{2} \log\left[K \int \rho(\varepsilon) e^{-2\varepsilon/T}\, d\varepsilon\right] \tag{19}$$

Which phase the system finds itself in is determined in the same way as in Section 2 [Eqs. (2)–(4)]: if $\lambda_{\min} < 1$, the system is always in phase II. If $1 < \lambda_{\min} < 2$, $\langle \log|Z_L| \rangle / L$ is given by the maximum of (17) and (18). If $\lambda_{\min} > 2$, $\langle \log|Z_L| \rangle / L$ is given by the maximum of (17) and (19).

The phase diagram for the case when the energy distribution is chosen to be a Gaussian,

$$\rho(\varepsilon) = \frac{1}{(2\pi)^{1/2}} \exp(-\varepsilon^2/2) \tag{20}$$

and $K=2$ is shown in Fig. 5. For this distribution the three possible expressions for $\langle \log|Z_L| \rangle / L$ are:

Phase I:

$$\frac{\langle \log|Z_L| \rangle}{L} = \frac{1}{2T^2} + \log K + \log(|1-2p|) \tag{21}$$

Phase II:

$$\frac{\langle \log|Z_L| \rangle}{L} = \frac{(2\log K)^{1/2}}{T} \tag{22}$$

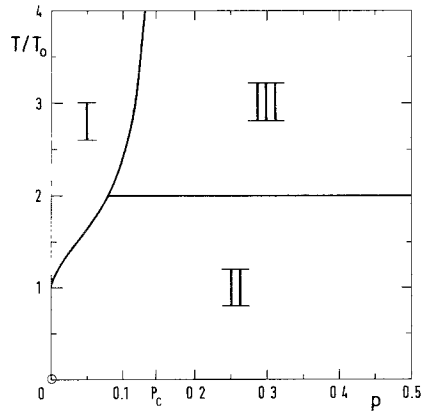

Fig. 5. Phase diagram for the mean field directed polymer problem with $K=2$ and Gaussian bonds [Eq. (20)], showing the positions of the three phases, Eq. (17)–(19). Here p_c shows the asymptotic position of the boundary between phases I and III when $T\to\infty$. The temperature scale is in units of $T_0=(2\log 2)^{-1/2}$.

Phase III:

$$\frac{\langle \log|Z_L|\rangle}{L}=\frac{1}{T^2}+\frac{1}{2}\log K \tag{23}$$

The relations for the transition lines are

$$\log|1-2p|=-\frac{1}{2}\left(\frac{1}{T}-\frac{1}{T_0}\right)^2 \qquad \text{for} \quad T\leqslant 2T_0 \tag{24}$$

$$\log|1-2p|=\frac{1}{2T^2}-\frac{1}{4T_0^2} \qquad \text{for} \quad T\geqslant 2T_0 \tag{25}$$

$$\log|1-2p|\leqslant -\frac{1}{8T_0^2} \qquad \text{for} \quad T=2T_0 \tag{26}$$

where $T_0=(2\log K)^{-1/2}$ is the transition temperature when $p=1$.

Notice that for all choices of $\rho(\varepsilon)$, the phase diagram remains symmetric about $p=1/2$. (This is due to the fact that the value of the energy ε on each bond and the sign S are uncorrelated.) Also, the transition between phases II and III is always second order, while the transitions between phases I and II and phases I and III are first order except at their endpoints, where they become second order.

Having presented our results and briefly discussed the nature of the three phases, let us compare our theoretical predictions with numerical

simulations. The simulations were performed in the following manner: Instead of directly simulating a tree structure (Fig. 4), which would be very difficult due to the exponential growth of the number of the bonds with the length of the polymer, we used the geometry discussed in Section 2 (see Fig. 3). We took the lattice which consists of L layers each containing N points. Each site at layer l is connected to K randomly chosen sites in layer $l+1$, the bonds being assigned random energies [Eq. (20)] and signs

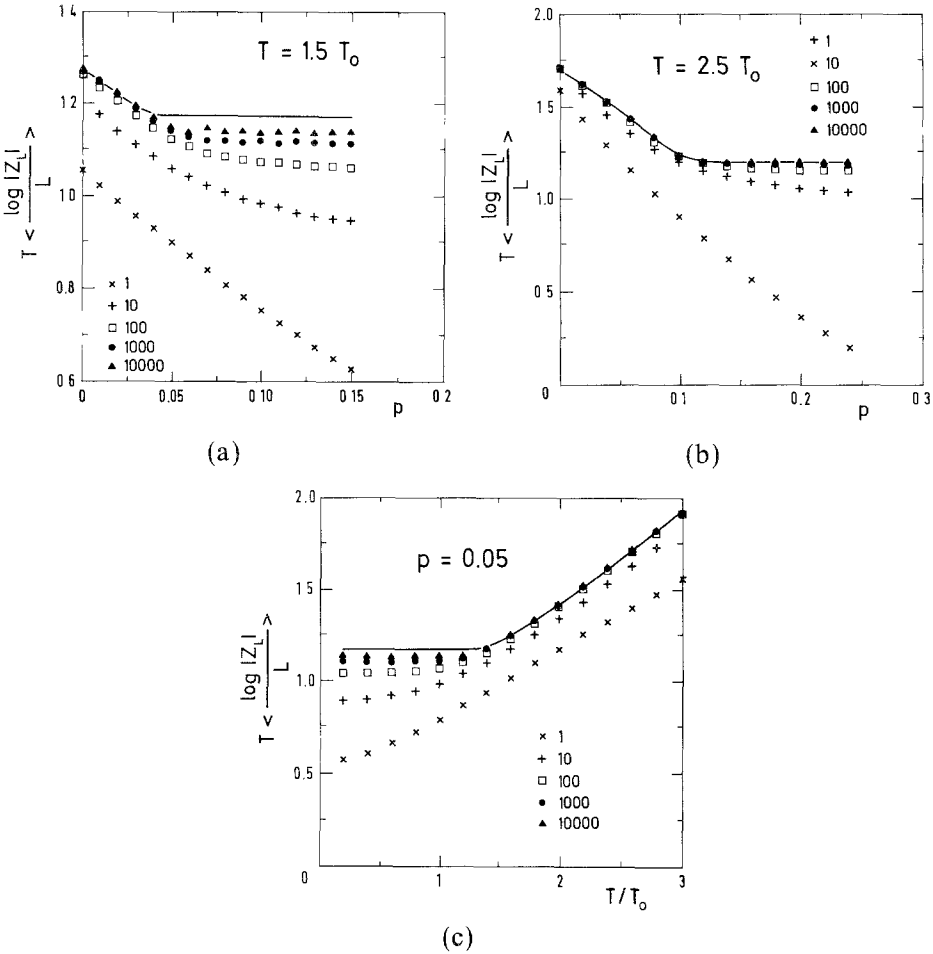

Fig. 6. Plot of $T\langle \log|Z_L|\rangle/L$ for the directed polymer problem in the geometry of Fig. 3, with $K=2$ and Gaussian bonds, along three lines on the phase diagram. The lines explored are (a) $T=1.5T_0$ and p varied, (b) $T=2.5T_0$ and p varied, (c) $p=0.05$ and T varied. The solid curves show the analytic predictions, Eqs. (17)–(19), and the points are the results of numerical simulations for $N=1$, 10, 100, 1000, 10,000.

as described above (plus with probability p and minus with probability $1-p$). If one keeps K fixed, as one increases the number of sites in each layer N, the structure will come to resemble locally that of a tree with branching ratio K. This procedure of keeping K fixed and examining how the simulations converge as N becomes large allows one to simulate much larger systems. The particular case we chose to look at was $K=2$ and Gaussian bonds, given by (20) (the phase diagram for this case is shown in Fig. 5). We took lengths of lattice $L=5\times10^5$ for $N=1$, $L=15\times10^4$ for $N=10$, $L=5\times10^4$ for $N=100$, $L=15\times10^3$ for $N=1000$, and $L=5\times10^3$ for $N=10{,}000$. In order to explore the phase diagram (Fig. 5), we selected three lines on the diagram along which to perform the simulations. The results of the simulations are shown, together with the theoretical predictions [see Eqs. (21)–(23) and Fig. 5] in Figs. 6a–6c. In Fig. 6a we show how $T\langle\log|Z_L|\rangle/L$ varies as one changes p at the temperature $T=1.5T_0$, and in Fig. 6b we show the same but at the temperature $T=2.5T_0$ [where $T_0=(2\log 2)^{-1/2}$]. Lastly, in Fig. 6c, we show how $T\langle\log|Z_L|\rangle/L$ varies with temperature when one fixes $p=0.05$. In all three cases one sees the first-order transition as a cusp in the "free energy." The numerical data converge well toward the theoretical results, giving good confirmation of our analytical expressions. As we remarked in the preceding section, one can see that the rate at which the numerical data converge toward the theoretical results is markedly better in the two high-temperature phases (I and III) than in the low-temperature phase (II).

4. THE RELATIONSHIP BETWEEN RANDOM MATRICES, DIRECTED POLYMERS, GREMs, AND REMs

Our main results have been presented in the two preceding sections. In the remainder of this paper, we shall explain how they were arrived at. To do this, it is necessary to notice the close relationship between four separate problems: the random matrix problem of Section 2, the directed polymer problem of Section 3, the generalized random energy model (GREM),[22,23] and the random energy model (REM).[24]

In Section 2 we have seen that calculating the Lyapunov exponent of large, sparse matrices gives the solution of the directed polymer in the layered geometry of Fig. 3. Indeed, if on each bond of this layered lattice, one chooses a random energy ε and a sign S, the matrix element x corresponding to this bond is just

$$x = S\exp(-\varepsilon/T) \tag{27}$$

as discussed at the end of Section 2.

As noticed in Section 3, if for the geometry of Fig. 3 one increases the number of points in each layer N while keeping the number of connections from each point to the next layer K fixed, the resulting structure begins locally to resemble a tree. Hence the problem of directed polymers on a Cayley tree (Fig. 4) will be recovered by taking N to be very large in the geometry of Fig. 3. This makes our first connection: if one can solve the problem on the tree (Section 3), one can calculate the largest Lyapunov exponent of the random matrices of Section 2, for N large via the identification (27).

In the way the polymer problem has been defined in Sections 2 and 3, the sign S and the energy ε are uncorrelated. This implies some constraint on the distribution $g(x)$ of the variable x obtained through the identification (27). In what follows we shall restrict our discussion to this case (S and ε uncorrelated) to keep the notation simpler. However, we have checked that the procedure can be extended to a general distribution $g(x)$.

We are now going to argue that the expression for $\langle \log |Z_L| \rangle / L$ for the tree geometry is the same as for two other problems, the REM and the GREM, that we shall solve in the next two sections. This identity between the tree, the REM, and the GREM was already known[15] in the case of positive weights,i.e., when all the signs $S = +1$. So the goal of the remainder of this work is to solve the REM and the GREM when the weights can have plus or minus signs and to argue that the identity with the tree problem remains valid.

4.1. The REM

In the random energy model REM, the partition function Z is defined as the sum of K^L independent terms

$$Z = \sum_{\mu=1}^{K^L} S_\mu \exp(-E_\mu/T) \tag{28}$$

where $S_\mu = \pm 1$ and $\exp(-E_\mu/T)$ are respectively the sign and the amplitude of the μth term of the sum.

The number K^L of terms in (28) is chosen to be the same as the number of polymers of length L on the tree; the random energy E_μ has the same distribution as the energy of a walk of L steps on the tree, i.e., its generating function is equal to

$$\langle e^{-\lambda E_\mu} \rangle = \langle e^{-\lambda \varepsilon} \rangle^L = \left[\int \rho(\varepsilon) e^{-\lambda \varepsilon} \, d\varepsilon \right]^L \tag{29}$$

where ε is the energy of a bond of the tree, and the sign S_μ has the same distribution as the sign of a given path of L steps on the tree, i.e.,

$$\begin{aligned} S_\mu &= +1 \qquad \text{with probability } \tfrac{1}{2}[1+(1-2p)^L] \\ S_\mu &= -1 \qquad \text{with probability } \tfrac{1}{2}[1-(1-2p)^L] \end{aligned} \tag{30}$$

For large L, the distribution $P(E)$ of E_μ takes in general the form

$$P(E) \simeq (2\pi L)^{-1/2}[-f''(E/L)]^{-1/2} \exp[Lf(E/L)] \tag{31}$$

where the function $f(x)$ is related to $\rho(\varepsilon)$ by a Legendre transform

$$\max_{\varepsilon} [f(\varepsilon) - \varepsilon\lambda] = \log\left[\int \rho(\varepsilon) e^{-\lambda\varepsilon}\, d\varepsilon\right] \tag{31a}$$

Using (29) and (31), one could show that the function f is convex ($f'' < 0$). For example, for a Gaussian $\rho(\varepsilon)$, one gets a Gaussian $P(E)$,

$$\rho(\varepsilon) = (2\pi)^{-1/2} \exp(-\varepsilon^2/2) \Rightarrow P(E) = (2\pi L)^{-1/2} \exp(-E^2/2L) \tag{32}$$

We see that the REM defined this way keeps the same number of terms in Z and the same distribution of single energies E as the tree problem. However, it neglects (as usual in the REM approach[24]) the correlations of energies or signs between different paths.

4.2. The GREM[22,23]

The generalized random energy model (GREM) aims to restore some of the correlations between energy levels or signs that have been ignored in the REM. In a GREM of n steps, the possible configurations of the system are represented by the endpoints of a tree of n steps (Fig. 7). The model is defined by two sets of n numbers, α_i, $1 \leqslant i \leqslant n$, and a_i, $1 \leqslant i \leqslant n$, which satisfy

$$\prod_{i=1}^{n} \alpha_i = K; \qquad \alpha_i > 1 \tag{33}$$

$$\sum_{i=1}^{n} a_i = 1; \qquad a_i > 0 \tag{34}$$

For each bond of the tree one chooses a random sign $\sigma_i^{(\mu)}$:

$$\begin{aligned} \sigma_i^{(\mu)} &= +1 \qquad \text{with probability } \tfrac{1}{2}[1+(1-2p)^{La_i}] \\ &= -1 \qquad \text{with probability } \tfrac{1}{2}[1-(1-2p)^{La_i}] \end{aligned} \tag{35}$$

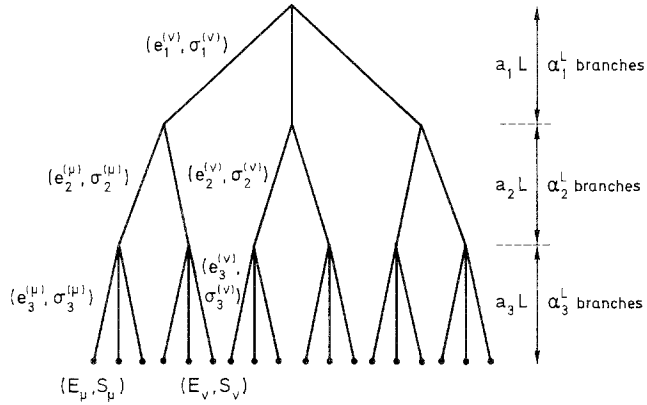

Fig. 7. The structure of a three-step ($n=3$) generalized random energy model (GREM).

and a random energy $e_i^{(\mu)}$ according to a distribution $P(e, a_i)$ which satisfies

$$\langle \exp(-\lambda e_i^{(\mu)}) \rangle = \left[\int \rho(\varepsilon) e^{-\lambda \varepsilon} \, d\varepsilon \right]^{La_i} \tag{36}$$

$$P(e, a_i) \sim \exp\left[La_i f\left(\frac{e}{La_i} \right) \right] \tag{37}$$

The total number of branches at level i is $(\alpha_1 \alpha_2 \cdots \alpha_i)^L$. By definition of the model, the configurations are identified with the endpoints of this tree and the energy E_μ and the sign S_μ associated with each configuration are given by

$$E_\mu = \sum_{i=1}^{n} e_i^{(\mu)} \tag{38}$$

$$S_\mu = \prod_{i=1}^{n} \sigma_i^{(\mu)} \tag{39}$$

where the sum and the product are over all the bonds which connect the configuration to the top of the tree.

In the case $n=1$, the GREM reduces to the REM. In the other limit ($n=L$; $a_i = 1/L$; $a_i = K^{1/L}$), one recovers the tree problem discussed in Section 3. So the GREM gives an interpolation between the REM and the tree. As long as n is finite, one can solve the GREM with similar ideas as those used in the solution of the REM. However, if n increases (choosing $a_i = 1/n$ and $\alpha_i = K^{1/n}$), the correlations between the energies E_μ and the signs S_μ of different configurations look more and more similar to those of the tree problem.

We shall see in Sections 5 and 6 that the REM and GREM (with $n=2$) have exactly the same phase diagram (Fig. 5) and the same expression for $\langle \log|Z_L| \rangle/L$ for L large. In fact, one can extend the results of Section 6 to arbitrary n. So the expression for $\langle \log|Z_L| \rangle/L$ is the same for the REM and the GREM (for any finite n) in the whole phase diagram.

In the case $p=0$, this common free energy of the REM and the GREM is known to be the same as the free energy of the tree problem.[15] Although we have been unable to derive the solution of the tree problem directly for $p \neq 0$, we believe that, since $\langle \log|Z_L| \rangle/L$ has the same expression for the GREM and the REM when one chooses the energy distributions, the signs, and the branching ratios to mimic the tree (35)–(37), this expression should remain valid for the tree problem.

So the problems (1) the Lyapunov exponent of the large, sparse random matrices, (2) the directed polymer on the tree, (3) the GREM and (4) the REM have the same solution (already given in Sections 2 and 3). The numerical simulations already presented in Sections 2 and 3 seem to confirm that we do indeed have the correct solution to all these four problems.

5. SOLUTION OF THE REM

In this section we solve the REM defined in the preceding section, (28). To recap, we have a system of K^L branches, each branch μ carrying a random energy E_μ chosen according to a distribution $P(E)$ given by (29), (31), and a random sign S_μ chosen according to (30). The partition function is then taken to be

$$Z_L = \sum_{\mu=1}^{K^L} S_\mu e^{-E_\mu/T} \tag{40}$$

where T is the temperature. To determine the phase diagram of the model, we are going to calculate the equivalent of the free energy, $-T\langle \log|Z_L| \rangle$.

One can divide Z_L into two parts: one part, Z_L^+, is the sum of the Boltzmann weights of all the branches with a positive sign S_μ, and the other, Z_L^-, is the sum of the Boltzmann weights of all the branches which have a negative sign,

$$Z_L = Z_L^+ - Z_L^- \tag{41}$$

Now we can solve the general problem provided that we know enough about the $p=0$ problem,[24] as Z_L^+ and Z_L^- are both $p=0$ REM partition functions.

5.1. The Case $p = 0$

To determine the phase diagram of the model (40), we shall need to know the solution of the $p = 0$ REM and also something about its sample-to-sample fluctuations. There are several ways[24–26] of solving the REM. We shall use here the intuitive one, which consists of using the micro-canonical ensemble.[24] If $\mathcal{N}(E)$ is the density of levels at energy E, the average of $\mathcal{N}(E)$ is given by [see (31)]

$$\langle \mathcal{N}(E) \rangle = (2\pi L)^{-1/2} [-f''(E/L)]^{-1/2} \exp[Lf(E/L)] K^L \tag{42}$$

Because the function f is convex, one expects that there are in general two energies E_{GS} and E'_{GS} ($E_{GS} < E'_{GS}$) for which $\langle \mathcal{N}(E) \rangle \simeq 1$. For energies such that $E/L < E_{GS}/L$ or $E/L > E'_{GS}/L$, the average $\langle \mathcal{N}(E) \rangle$ is exponentially small in L. Therefore

$$\mathcal{N}_{\text{typical}}(E) = 0 \tag{43}$$

For energies such that $E_{GS}/L < E/L < E'_{GS}/L$, the average $\langle \mathcal{N}(E) \rangle$ is exponentially large in L. Therefore the typical value is the same as the average,

$$\mathcal{N}_{\text{typical}}(E) = \langle \mathcal{N}(E) \rangle \pm \langle \mathcal{N}(E) \rangle^{1/2} \tag{44}$$

Lastly, for energies E which (for large L) differ from E_{GS} or E'_{GS} by order 1, $\mathcal{N}_{\text{typical}}(E)$ is of order 1 and the fluctuations are also of order 1 [so (44) still gives the magnitude of the typical value and of the typical fluctuations].

From (43) and (44) one can obtain the large-L behavior and fluctuations of the partition function

$$Z_L = \int \mathcal{N}_{\text{typical}}(E) \exp(-E/T)\, dE \tag{45}$$

First, the ground-state energy E_{GS}/L is given by the condition $\langle \mathcal{N}(E) \rangle = 1$, i.e., is the lower solution of

$$f(E_{GS}/L) = -\log K \tag{46}$$

where the function f is defined by (31) and (29). The transition temperature occurs at T_c given by

$$f'(E_{GS}/L) = 1/T_c \tag{47}$$

Above T_c, the integral (45) is dominated by energies E where $\langle \mathcal{N}(E) \rangle$ is very large, i.e., the free energy for $T > T_c$ is given by [see (31a)]

$$\lim_{L \to \infty} \frac{\langle \log Z_L \rangle}{L} = \max_{\varepsilon} [f(\varepsilon) - \varepsilon/T] + \log K$$

$$= \log \left[K \int \rho(\varepsilon) \exp\left(-\frac{\varepsilon}{T}\right) d\varepsilon \right]$$

$$= \lim_{L \to \infty} \frac{\log \langle Z_L \rangle}{L} \tag{48}$$

For $T < T_c$ the integral (45) is dominated by energies close to E_{GS} (since for $E/L < E_{GS}/L$ one has $\mathcal{N}_{\text{typical}} = 0$). Therefore

$$\lim_{L \to \infty} \frac{\langle \log Z_L \rangle}{L} = \lim_{L \to \infty} \frac{-E_{GS}}{L} \frac{1}{T} \tag{49}$$

This reasoning can be easily generalized to calculate the typical fluctuations of the partition function. Using the fact the fluctuations of $\mathcal{N}(E)$ are given by (44), one finds that the magnitude of the fluctuations changes at $2T_c$. Thus, one obtains:

For $T < T_c$

$$Z_L(T) = a(T) \exp\left(\frac{-E_{GS}}{T}\right) \tag{50}$$

For $T_c < T < 2T_c$

$$Z_L(T) = \langle Z_L(T) \rangle \pm a(T) \exp\left(\frac{-E_{GS}}{T}\right)$$

$$= K^L \left\langle \exp -\frac{\varepsilon}{T} \right\rangle^L \pm a(T) \exp\left(\frac{-E_{GS}}{T}\right) \tag{51}$$

For $T > 2T_c$

$$Z_L(T) = \langle Z_L(T) \rangle \pm a(T) \langle Z_L(T/2) \rangle^{1/2}$$

$$= K^L \langle \exp(-\varepsilon/T) \rangle^L \pm a(T)\, K^{L/2} \langle \exp(-2\varepsilon/T) \rangle^{L/2} \tag{52}$$

where in (50)–(52), $a(T)$ is a quantity which has sample-to-sample fluctuations of order one. The appearance of the temperature $2T_c$ is simply due to the fact that

$$\int_{E_{GS}} \langle \mathcal{N}(E) \rangle^{1/2} \exp(-E/T)\, dE \tag{53}$$

is dominated by energies where $\langle \mathcal{N}(E) \rangle$ is large when $T > 2T_c$, whereas it is dominated by the neighborhood of $E = E_{GS}$ when $T < 2T_c$.

5.2. The Case $p \neq 0$

We noticed in (41) that one could write Z_L as the difference of two $p = 0$ REM partition functions, Z_L^+ and Z_L^-. Since the random signs are chosen according to (30), we know that Z_L^+ and Z_L^- are the sum of

$$\frac{K^L}{2} [1 \pm (1-2p)^L \pm cK^{-L/2}] \tag{54}$$

terms, respectively, where c is a sample-dependent number of order 1.

Using the results (51)–(54) for Z_L^+ and Z_L^-, one finds that:

For $T < T_c$

$$Z_L = Z_L^+ - Z_L^- \sim a(T) \exp(-E_{GS}/T) \tag{55}$$

For $T_c < T < 2T_c$

$$Z_L = Z_L^+ - Z_L^- \simeq K^L \langle \exp(-\varepsilon/T) \rangle^L (1-2p)^L \pm a(T) \exp(-E_{GS}/T) \tag{56}$$

For $2T_c \leqslant T$

$$Z_L = Z^+ - Z_L^- = K^L \langle \exp(-\varepsilon/T) \rangle^L (1-2p)^L \pm a(T)\, K^{L/2} \langle \exp(-2\varepsilon/T) \rangle^{L/2} \tag{57}$$

The main difference between (56)–(57) and the case $p = 0$, (51)–(52), is that in (51) and (52) the fluctuating part was negligible compared with the leading term $\langle Z_L(T) \rangle$. In (56)–(57), the effect of the signs has been to reduce the average $\langle Z_L(T) \rangle$ by the factor $(1-2p)^L$, whereas the magnitude of the fluctuations is not affected by the signs. Therefore, depending on the temperature T and p, the term which dominates (56) and (57) is either the term coming from the average or the fluctuating term. This leads to the three following possible expressions for the free energy:

Phase I:

$$\lim_{L \to \infty} \frac{\log |Z_L|}{L} = \log \left[K \left\langle \exp\left(-\frac{\varepsilon}{T}\right) \right\rangle |1-2p| \right] \tag{58}$$

Phase II:

$$\lim_{L \to \infty} \frac{\log |Z_L|}{L} = \frac{-E_{GS}}{T} \tag{59}$$

Phase III:

$$\lim_{L\to\infty}\frac{\log|Z_L|}{L}=\frac{1}{2}\log\left[K\left\langle\exp\left(\frac{-2\varepsilon}{T}\right)\right\rangle\right] \tag{60}$$

and to the facts that (a) for $T<T_c$, the system is always in phase II, (b) for $T_c<T<2T_c$, the system is either in phase II or I, depending on what is the better free energy, and (c) for $T>2T_c$, the system has to choose between phase I and phase III, again according to what is the better free energy.

Notice that for (58)–(60) to coincide with (17)–(19) one needs to show that (59) and (18) are the same. To do so, one can rewrite the relation (31a) between the function f and the distribution $\rho(\varepsilon)$:

$$\max_{\varepsilon}\left(f(\varepsilon)-\varepsilon\lambda+\log K\right)=\log\left[K\int\rho(\varepsilon)e^{-\lambda\varepsilon}\,d\varepsilon\right] \tag{61}$$

From (61), it is possible to see that if ε_0 is the value of ε which maximizes the left-hand side of (61), one has

$$f(\varepsilon_0)+\log K=\left(1-\lambda\frac{d}{d\lambda}\right)\log\left[K\int\rho(\varepsilon)e^{-\lambda\varepsilon}\,d\varepsilon\right] \tag{62}$$

Therefore, if $\lambda_{\min}$ is the value of λ which minimizes

$$\frac{1}{\lambda}\log\left[K\int\rho(\varepsilon)e^{-\lambda\varepsilon}\,d\varepsilon\right] \tag{63}$$

one can see that the right-hand side of (62) vanishes for $\lambda=\lambda_{\min}$. So the corresponding energy ε_0 satisfies

$$f(\varepsilon_0)+\log K=0 \tag{64}$$

i.e., ε_0 is the ground-state energy [see (46)].

6. SOLUTION OF THE TWO-STEP GREM

In Section 4 we defined a GREM of n steps. We shall now show how one can solve the case when $n=2$. We have a two-step tree structure with branching ratios α_1^L and α_2^L at the first and second steps, respectively, and we shall choose that $\alpha_1\alpha_2=K$ [see (33)]. On each branch of the tree one places a random energy $e_i^{(\mu)}$ chosen from the probability distribution (37) and a random sign $\sigma_i^{(\mu)}$ chosen according to

$$\begin{aligned}\sigma_i^{(\mu)}&=+1 \qquad \text{with probability } \tfrac{1}{2}[1+q_i^L(e_i^{(\mu)})]\\ &=-1 \qquad \text{with probability } \tfrac{1}{2}[1-q_i^L(e_i^{(\mu)})]\end{aligned} \tag{65}$$

Here we have allowed the sign distributions to depend on the energy. The case of uncorrelated sign and energy distribution (35) is recovered by choosing $q_i = (1-2p)^{a_i}$. The sign S_μ and energy E_μ of each configuration μ associated with one endpoint of the tree are defined as in (38) and (39) and one then defines the partition function to be

$$Z = \sum_{\mu=1}^{K^L} S_\mu \exp\left(\frac{-E_\mu}{T}\right) \tag{66}$$

This problem has already been solved when all the signs are all chosen to be the same.[22,23] We shall now extend this solution to the more general case (65).

The average number of first step branches with a sign σ_1 and an energy e_1, $\langle \mathcal{N}_1^{\sigma_1}(e_1) \rangle$, is given by

$$\langle \mathcal{N}_1^{\sigma_1}(e_1) \rangle \sim [1 + \sigma_1 q_1^L(e_1)] \exp\left[L\left(a_1 f\left(\frac{e_1}{La_1}\right) + \log \alpha_1 \right)\right] \tag{67}$$

where we have used the energy distribution (37). The function f is convex and so one expects that there are two energies e_{GS} and e'_{GS} ($e_{GS} < e'_{GS}$) for which $\langle \mathcal{N}_1^{\sigma_1}(e_1) \rangle \sim 1$. For energies below e_{GS} or above e'_{GS} the average (67) is exponentially small in L. Hence,

$$\mathcal{N}_{1,\text{typical}}^{\sigma_1}(e_1) = 0 \tag{68}$$

For energies between e_{GS} and e'_{GS}, $\langle \mathcal{N}_1^{\sigma_1}(e_1) \rangle$ is exponentially large in L and so

$$\mathcal{N}_{1,\text{tyical}}^{\sigma_1}(e_1) = \langle \mathcal{N}_1^{\sigma_1}(e_1) \rangle + c^{\sigma_1}(e_1) \langle \mathcal{N}_1^{\sigma_1}(e_1) \rangle^{1/2} \tag{69}$$

where $c^{\sigma_1}(e_1)$ is a Gaussian fluctuation of order one.

Knowing the typical values of $\mathcal{N}_1^{\sigma_1}(e_1)$, one can then calculate the average number of configurations with energy E and sign σ_1 on step one and σ_2 on step two, $\langle \mathcal{N}^{\sigma_1,\sigma_2}(E) \rangle$, given that $\mathcal{N}^{\sigma_1}(e)$ is given by its typical value (68)–(69),

$$\langle \mathcal{N}^{\sigma_1,\sigma_2}(E) \rangle \sim \int de\, \mathcal{N}_1^{\sigma_1}(e)_{\text{typical}} [1 + \sigma_2 q_2^L(E-e)]$$

$$\times \exp\left[L\left(\log \alpha_2 + a_2 f\left(\frac{E-e}{La_2}\right)\right)\right] \tag{70}$$

So, using (68) and (69),

$$\langle \mathcal{N}^{\sigma_1,\sigma_2}(E)\rangle \sim \int_{e_{GS}<e<e'_{GS}} de \left\{ [1+\sigma_1 q_1^L(e)] \times \exp\left[L\left(\log \alpha_1 + a_1 f\left(\frac{e}{La_1}\right)\right)\right] + c^{\sigma_1}(e) \times \exp\left[\frac{L}{2}\left(\log \alpha_1 + a_1 f\left(\frac{e}{La_1}\right)\right)\right]\right\} \times [1+\sigma_2 q_2^L(E-e)] \exp\left[L\left(\log \alpha_2 + a_2 f\left(\frac{E-e}{La_2}\right)\right)\right] \tag{71}$$

The integral in (71) can be done by a saddle method. One replaces each integral by the integrand evaluated either at its saddle point, if the saddle point lies within the allowed range, or at the boundary, if the saddle point falls outside the range of integration. From its average (71), one can then determine the typical value of $\mathcal{N}^{\sigma_1,\sigma_2}(E)$ as we did before for $\mathcal{N}_1^{\sigma_1}(e_1)$, i.e.,

$$\begin{aligned} &\mathcal{N}^{\sigma_1,\sigma_2}(E)_{\text{typical}} \\ &\quad = 0 && \text{if} \quad \langle \mathcal{N}^{\sigma_1,\sigma_2}(E)\rangle \ll 1 \\ &\quad = \langle \mathcal{N}^{\sigma_1,\sigma_2}(E)\rangle + d^{\sigma_1,\sigma_2}(E)\langle \mathcal{N}^{\sigma_1,\sigma_2}(E)\rangle^{1/2} && \text{if} \quad \langle \mathcal{N}^{\sigma_1,\sigma_2}(E)\rangle \gg 1 \end{aligned} \tag{72}$$

where $d^{\sigma_1,\sigma_2}(E)$ is a fluctuating quantity of order one. The total density of levels $\mathcal{N}(E)$ weighted by the signs can then be evaluated by summing over the contributions from each $\mathcal{N}^{\sigma_1,\sigma_2}$:

$$\mathcal{N}(E)_{\text{typical}} = \sum_{\sigma_1,\sigma_2=\pm 1} \sigma_1\sigma_2 \mathcal{N}^{\sigma_1,\sigma_2}(E)_{\text{typical}} \tag{73}$$

As expression (71) is rather cumbersome, let us from now on limit ourselves to considering the case

$$f(x) = -\frac{x^2}{2}; \qquad q_i(e) = (1-2p)^{a_i}; \qquad a_i = \frac{\log \alpha_i}{\log K} \tag{74}$$

For this choice one obtains that

$$\mathcal{N}(E)_{\text{typical}} = (1-2p)^L K^L \exp\left[\frac{-e^2}{2La_1} - \frac{(E-e)^2}{2La_2}\right] + d(E) K^{L/2} \exp\left[\frac{-e^2}{4La_1} - \frac{(E-e)^2}{4La_2}\right] \tag{75}$$

where

$$\begin{aligned} e &= a_1 E \qquad \text{if} \quad \left|\frac{E}{L}\right| < \left(\frac{2\log \alpha_1}{a_1}\right)^{1/2} \\ e &= L(2a_1 \log \alpha_1)^{1/2} \qquad \text{otherwise} \end{aligned} \tag{76}$$

and $d(E)$ is a fluctuating quantity of order 1 and therefore such that

$$\lim_{L\to\infty} \frac{1}{L} \log d(E) \to 0$$

Also if (75) gives an exponentially small value, one must take $\mathcal{N}(E)_{\text{typical}} = 0$.

For this particular choice of energy and sign distribution (74) chosen to mimic the tree, one finds that (75) and (76) lead to $\mathcal{N}(E)_{\text{typical}}$ of the form shown in Fig. 8.

Knowing $\mathcal{N}(E)_{\text{typical}}$, one can calculate the typical value of the partition function using the relation

$$Z(T) = \int dE\, \mathcal{N}(E) e^{-E/T} \tag{77}$$

Evaluating this integral by taking a saddle point corresponds to identifying $1/T$ with the slope of the curve $\log \mathcal{N}(E)$. One can see that this leads to two phases separated by a second-order transition when $\log \mathcal{N}(E)$ has the form shown in Fig. 8a.

When $\log \mathcal{N}(E)$ has the form of Fig. 8b one can obtain three phases with the two high-temperature phases separated by a first-order transition.

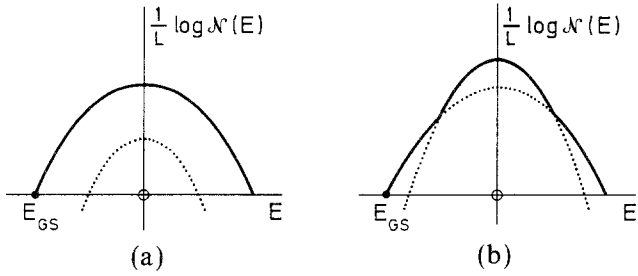

Fig. 8. The solid line shows the shape of $[\log \mathcal{N}(\varepsilon)_{\text{typical}}]/L$ for the two-step GREM of Section 6 for two values of p: (a) if $\log|1-2p| < -\frac{1}{2}\log K$ and (b) if $-\frac{1}{2}\log K < \log|1-2p|$. In (a) $\mathcal{N}_{\text{typical}}(\varepsilon)$ is dominated at all energies by fluctuations. In (b) there are three regions: the middle one where $\mathcal{N}_{\text{typical}}(\varepsilon)$ is equal to $\langle \mathcal{N}(\varepsilon) \rangle$ and the side ones where $\mathcal{N}_{\text{typical}}(\varepsilon)$ is dominated by fluctuations.

This corresponds geometrically to the existence of a straight line that is tangent to $\log \mathcal{N}(E)$ at two points. Carrying out this procedure for all values of p, one sees that this two-step GREM has the same free energy phase diagram as that of the corresponding REM [see (58)–(60)] with a Gaussian distribution of energies (20).

This calculation on the GREM of two steps ($n=2$) can be extended without any difficulty to any other value of n. The result is that the phase diagram and the expressions [(58)–(60)] are the same for all values of n ($n=1, 2,...$). Thus, we conclude that the GREM with an arbitrary number n of steps has the same free energy as the REM and since for n large, the GREM looks more and more like the tree, we conjecture that the tree problem of Section 3 and the REM have the same solution.

The reasoning of this section can be extended easily to functions f more general than that of (74). Also, if, instead of random signs on each bond of the tree, we had some complex phases, i.e., $\sigma=\exp(i\varphi)$ with φ random, the reasoning of Sections 5 and 6 would remain unchanged and one would conclude that the REM and the tree still have the same free energies.

One way of seeing it is to consider cases where the allowed phases take a discrete set of values (the n roots of unity). Then, instead of distinguishing between Z_L^+ and Z_L^-, one has to consider $Z_L^{(j)}$ for each possible phase $\exp(2i\pi j/n)$. The effect of competition between the fluctuations and the average would remain the same.

Of course, if we had made more general choices of the a_i and of the α_i (which would not mimic the tree), then the final results would depend on n and on these choices of the a_i and α_i as is the case for the GREM when $p=0$.[22,23]

7. CONCLUSION

In this paper, we have obtained the solution of four different problems.

In Section 2, we gave a formula for the largest Lyapunov exponent of a product of large, sparse, real random matrices [Eqs. (2)–(7)]. The result is valid for an arbitrary distribution $g(x)$ (which does not contain δ functions) of the nonzero elements, provided they are independent and identically distributed. In Section 3 we presented expressions for the free energy of the polymer in a random medium [(17)–(19)] generalized to include random signs in the mean field limit (i.e., when the polymer is drawn on a tree).

Although we could not solve these two problems directly, we argued in Section 4 that these two problems have the same free energy as the REM and the GREM (the similarity between the REM, the GREM, and the

polymer on a tree was already known[15] in the case of $p=0$) that we solved in Sections 5 and 6. Our numerical simulations of Sections 2 and 3 gave good confirmation of our expressions for the Lyapunov exponent.

The problem of directed polymers in a random medium generalized to include random signs[21] has recently been the topic of some controversy. The debate centers around whether, in finite dimension, the addition of random signs into the problem changes the exponents that characterize the fluctuations of $\log Z$ and the transverse fluctuations. In $1+1$ dimensions these exponents are known exactly for the standard directed polymer.[13,14] However, recent numerical simulations[27,28] and analytic arguments[27,29,30] give conflicting results for whether these exponents remain true for the case of random signs. Our results cannot settle this debate one way or the other. We can, however, conclude from our results that a new phase (phase III) appears at the mean field level which is not present when there are no random signs. Whether this new phase persists in dimension $1+1$, and, if it does, whether it would lead to different exponents, we cannot say.

At the end of this paper, several interesting questions remain to be answered. First, it would be nice to be able to derive directly the results of Sections 2 and 3 without using the arguments of Section 4. Starting from the mean field solution of Section 3, one could also try to develop a $1/d$ expansion method as was done for the directed polymer problem with positive weights.[17] One can also wonder what would be the critical dimensions of the different phases (I, II, and III) which exist at the mean field level. One knows that for $p=0$,[16] phase I disappears in dimension less than 2. Does this remain true for phase III when $p \neq 0$?

For the problem of random matrices discussed in Section 2, the first question would be to try to see whether one could calculate all the other Lyapunov exponents. It would also be interesting to understand why the convergence in the limit $N \to \infty$ seems to be always very quick in phases I and III and slower in phase II. Lastly, products of random matrices[31] have often been considered in the context of localization. Although the sparse matrices we consider here (in Section 2) are probably not directly related to a precise model of localization, one can wonder whether for products of random matrices which describe in a more realistic way a localization problem, there would remain a trace of the three phases that we have described in Section 2 and, if so, what would be the physical interpretation of these three phases.

ACKNOWLEDGMENTS

J. C. acknowledges support from the SERC. B. D. thanks T. Spencer for his kind hospitality at the Institute for Advanced Study, where this

work was started. We also thank C. M. Newman, Y. Shapir, and A. S. Sznitman for useful discussions.

REFERENCES

1. E. P. Wigner, *Ann. Math.* **62**:548 (1955); **65**:203 (1957); **67**:325 (1958).
2. F. J. Dyson, *J. Math. Phys.* **3**:140, 157, 166, 1191, 1199 (1962).
3. M. L. Mehta, *Random Matrices and the Statistical Theory of Energy Levels* (Academic Press, New York, 1967).
4. F. J. Dyson, *Phys. Rev.* **92**:1331 (1953).
5. S. Alexander, J. Bernasconi, W. R. Schneider, and R. Orbach, *Rev. Mod. Phys.* **53**:175 (1981).
6. J. P. Eckmann and D. Ruelle, *Rev. Mod. Phys.* **57**:617 (1985).
7. R. Livi, A. Politi, S. Ruffo, and A. Vulpiani, *J. Stat. Phys.* **46**:1947 (1987).
8. B. Derrida, K. Mecheri, and J. L. Pichard, *J. Phys.* (Paris) **48**:733 (1987), and references therein.
9. B. Derrida, M. Mendès-France, and J. Peyrière, *J. Stat. Phys.* **45**:314, 439 (1986).
10. C. M. Newman, *Commun. Math. Phys.* **103**:121 (1986).
11. C. M. Newman, *Contemp. Math.* **50**:121 (1986).
12. M. Kardar and Y. C. Zhang, *Phys. Rev. Lett.* **58**:2087 (1987).
13. M. Kardar, *Nucl. Phys. B* **290**:582 (1987).
14. D. A. Huse, C. L. Henley, and D. S. Fisher, *Phys. Rev. Lett.* **55**:2924 (1985).
15. B. Derrida and H. Spohn, *J. Stat. Phys.* **51**:817 (1988).
16. J. Cook and B. Derrida, *J. Stat. Phys.* **57**:89 (1989).
17. J. Cook and B. Derrida, *J. Phys. A* **23**:1523 (1990).
18. W. Renz, to be published.
19. V. L. Nguyen, B. Z. Spivak, and B. I. Shklovskii, *JETP Lett.* **41**:42 (1985).
20. V. L. Nguyen, B. Z. Spivak, and B. I. Shklovskii, *JETP Sov. Phys.* **62**:1021 (1985).
21. Y. Shapir and X. R. Wang, *Europhys. Lett.* **4**:1165 (1987).
22. B. Derrida, *J. Phys. Lett.* (Paris) **46**:L401 (1985).
23. B. Derrida and E. Gardner, *J. Phys. C* **19**:2253, 5783 (1986).
24. B. Derrida, *Phys. Rev. B* **24**:2613 (1981).
25. D. Ruelle, *Commun. Math. Phys.* **198**:225 (1987).
26. A. Galves, S. Martinez, and P. Picco, *J. Stat. Phys.* **54**:112, 515 (1989).
27. E. Medina, M. Kardar, Y. Shapir, and X. R. Wang, *Phys. Rev. Lett.* **62**:941 (1989).
28. Y. C. Zhang, *Phys. Rev. Lett.* **62**:979 (1989).
29. Y. C. Zhang, *Europhys. Lett.* **9**:113 (1989).
30. Y. C. Zhang, *J. Stat. Phys.* **57**:1123 (1989).
31. J. L. Pichard and G. Sarma, *J. Phys. C* **14**:L127, L617 (1981).